Materials Science in Semiconductor Processing 16 (2013) 1753–1758

Contents lists available at SciVerse ScienceDirect

Materials Science in Semiconductor Processing

journal homepage: www.elsevier.com/locate/mssp

Chemical bath deposition of nanocrystalline ZnS thin films: Influence of pH on the reaction solution

H. Lekiket, M.S. Aida *

Laboratoire Couches Minces et Interfaces Faculté de Sciences Université de Constantine, 25000 Constantine, Algerie

ARTICLE INFO

Available online 20 July 2013

Keywords:
II–VI semiconductor
Chemical bath
Thin films

ABSTRACT

Zinc sulfide (ZnS) thin films were deposited onto glass substrates using chemical bath deposition technique (CBD). The deposition were carried out in a bath solution with pH ranged from 9 to 11. X-ray diffraction (XRD) and atomic force microscopy (AFM) were used to characterize the films structure and morphology respectively. The amorphous structure of as-deposited films is converted to a nanocrystalline one after a thermal annealing at 550 °C. The deposited ZnS films exhibit a high optical transmission in the UV–visible range (≥80%). They have a direct band gap. Using a solution with pH equal to 10 yields to films with larger optical band gap, smoother surface and lower electrical conductivity.

1. Introduction

Zinc sulfide thin film is an important semiconductor material with large band gap (3.68 eV) [1,2], relatively high refractive index [3] and high transmittance in the visible range [4]. These properties are promising for short wavelength optoelectronic device applications, such as electroluminescent devices [5,6] and antireflection coating for solar cells [7]. The most important application of ZnS is an environmental friendly buffer layer in CuIn(Ga)Se (CIGS) based solar cell [8]. Despite using CdS success as buffer layer in CIGS based solar cells, comforted by the 19.5% efficiency recorded in this structure [9], there is a toxic hazards when using this material. This stimulates research towards developing a Cd free buffer layer. For this purpose; ZnS has emerged as an alternative candidate. Moreover, the advantage of ZnS by comparison to CdS is its wider band gap which results in transmitting more high-energy photons towards the junction. This enhances the cells blue response. Thereafter, a considerable progress of using ZnS in CIGS thin film solar cells has been achieved. This efforts yields to an efficiency up to 18.6% achieved in ZnO/ZnS/CIGS solar cells [10].

Various techniques such as thermal evaporation [11] molecular beam epitaxy [12], pulsed electrochemical deposition [13], photochemical deposition [14], sputtering [15], metal organic vapor phase epitaxy [16], spray pyrolysis [17], and atomic layer deposition [18] have been employed to synthesize ZnS thin films. However, Chemical Bath Deposition (CBD) appears as an interesting technique for ZnS thin films deposition. CBD technique is the most convenient, reliable, simplest, inexpensive method and useful for large area preparation of thin films at temperature close to room temperature [16,17]. CBD technique is based on the controlled precipitation from solution of a deposit on a substrate. The use of a complexing agent is very useful to control the precipitation on a solid surface and to avoid the powder formation in the bath solution. Several studies have been carried to investigate the influence of different bath solution parameters such as complexing agent [19–22], solution and annealing temperature [23–26], salts source and molarity [25,27]. However, few studies have been devoted to the study of solution pH influence [28].

The aim of this paper deals with the preparation of ZnS thin films using chemical bath deposition technique. The effect of solution pH on structure; morphology and electrical conductivity of ZnS thin films was investigated.

2. Experimental details

The used bath solution for film deposition were prepared with a stirred aqueous solutions containing zinc

* Corresponding author. Tel.: +213 663146426.
E-mail address: aida_salah2@yahoo.fr (M.S. Aida).

1369-8001/$ - see front matter © 2013 Elsevier Ltd. All rights reserved.
http://dx.doi.org/10.1016/j.mssp.2013.06.028

sulfate ($ZnSO_4 \cdot 7H_2O$), thiourea ($CS(NH_2)_2$); 33% ammonia solution (NH_4OH) and hydrazine hydrate (N_2H_4). The pH of the as prepared solution is larger than 11. While, chemical bath deposition process requires a pH solution in the range of 9–11, thereafter, we have adjusted the solution pH to the required value by addition of hydrochloride acid drops. The solution temperature was maintained at 80 °C. Substrates were removed from the deposition bath after the desired time, rinsed with deionized water and dried in air. The deposited films thicknesses are ranged from 54 nm to 122 nm,the deposition time was fixed at 1 h. The films thicknesses were determined by the stylus displacement of a profilometer Dektak 3ST. The XRD spectra were obtained by means of Bruker AXS D8 Advance using Cu Kα monochromatic radiations. The wavelength, accelerating voltage and current were, respectively, 1.5418 Å, 40 KV and 30 mA. Atomic force microscopy (AFM) observations were carried out with a Veecoo Dimension 3100 Atomic Force Microscopy. The optical characterization of films was carried by means of transmittance measurements with a double-beam spectrophotometer (UV-3101 PC-Shimadzu) to determine films band gap energy. Two probes method is used for films conductivity determination since it is the most suitable for electrical measurements of highly resistive materials. The conductivity measurements were performed in the dark condition at the room temperature using gold (Au) metal contacts. The current was measured using a Keithley 617 electrometer.

3. Results and discussion

3.1. Growth rate

In Fig. 1 we have reported the variation of ZnS films deposition rate as a function of pH solution. The deposition rate is equal to the ratio between film thickness and deposition time. As seen, the deposition rate depends on pH solution, it varies from 0.9 nm/s to 2 nm/s, the lower deposition rate is measured in film prepared with a pH equal to 10. This low deposition rate can be due to the higher ZnS solubility at this pH. Hubert et al. [29] in a thermodynamic study, have calculated ZnS solubility in an ammonia solution, they reported a maximal solubility at pH = 10. Hence a small amount of the deposited film is dissolved and released to the solution at this pH condition resulting in films thickness reduction. In general, the obtained deposition rate is relatively low, this is due to the large stability constant of $ZnSO_4$ salt used as source of Zn in the present study. Ernits et al. [30] have investigated the influence of anion from zinc salt nature, they concluded that $ZnSO_4$ yields to the lower ZnS deposition rate due to its higher stability constant pK_1 ($pK_1 = 2,3$).

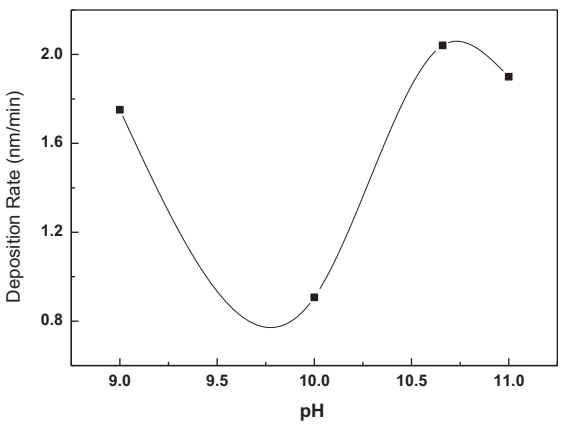

Fig. 1. Variation of ZnS thin films deposition rate as a function of pH solution.

ZnS thin film deposition by the CBD method involves several chemical reactions. In the solution, $ZnSO_4$ is divided into two separate ions according to:

$$ZnSO_4 \rightarrow Zn^{2+} + SO_4^{2-} \quad (1)$$

The decomposition of the thiourea is given by:

$$CS(NH_2)_2 + OH^- \rightarrow SH^- + CH_2N_2 + H_2O \quad (2)$$

In the solution, ammonia is in equilibrium with ammonium hydroxide which provide hydroxide ions OH^- for thiourea decomposition in S^{2-} ions and NH_3 for Zn ligand formation according to the following equations:

$$NH_4^+ + OH^- \leftrightarrow NH_3 + H_2O \quad (3)$$

$$SH^- + OH^- \leftrightarrow S^{2-} + H_2O \quad (4)$$

$$Zn^{2+} + NH_3 \rightarrow Zn[NH_3]^{2+} \quad (5)$$

The sulfide and complexes ions migrate to the substrate surface to form ZnS deposit according to:

$$Zn[NH_3]^{2+} + S^{2-} \rightarrow ZnS + NH_3 \quad (6)$$

Hydrazine ($N_2H_4\ H_2O$) has been also added to the bath to promote the ZnS formation. At temperature (80 °C), it dissociates and supplies more necessary OH^- ions for S^{2-} ions formation. Several researchers have reported the use of hydrazine hydrate in the chemical bath [31–34]. Lincot et al. suggested that the addition of hydrazine is not essential for the growth of ZnS, but it improves homogeneity and the growth rate of films [31]. The pH solution can be controlled by hydrazine addition. With increasing hydroxide ions OH^- concentration the solution pH is enhanced. As can be seen in Fig. 1, the influence of pH on the deposition rate can be divided in two regions:

- for pH < 10 the deposition rate is reduced with pH increasing, this can be due to the concurrence between the ligand $Zn[NH_3]^{2+}$ formation (Eq. (5)) and $Zn(OH)_2$ precipitation according to the equation:

$$Zn^{2+} + 2OH^- \rightarrow Zn(OH)_2 \quad (7)$$

- for pH > 10, ion hydroxide concentration is sufficiently large to promote the formation of ZnS according the Eqs. (3)–(6), and thereafter the observed increase in the deposition rate.

3.2. Structural properties

Fig. 2(a) shows X-ray diffraction pattern of as-deposited ZnS thin films. These patterns do not reveal any well defined peaks indicating that the as-deposited films of ZnS deposited by the solution growth technique are amorphous material in nature. This is in agreement with several authors results [2,35,36]. It is well known that ZnS films prepared by CBD technique, when using popular complexing agent such as ammonia and hydrazine, are either amorphous or poorly crystallized. Therefore, annealing is generally needed to improve films crystallinity [37,38]. However, well-crystallized phase pure ZnS thin films were directly prepared at a temperature of 80 °C by CBD by using tri-sodium citrate as the complexing agent [39].

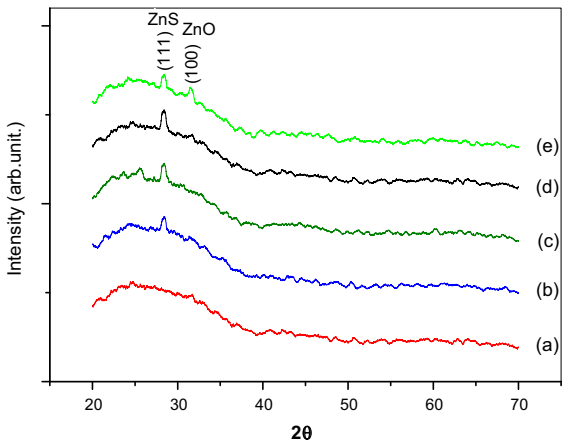

Fig. 2. X-ray diffractograms of thin films (a) as-deposited and after thermal annealing of ZnS films prepared with different pH (b) pH=9, (c) pH=10, (d) pH=10.66 and (e) pH=11.

After annealing in an open oven at 550 °C during 2 h, XRD films pattern exhibits a single peak located at $2\theta=28.4^{\circ}$ (Fig. 2b–e). The latter is assigned to the (111) direction corresponding to the cubic structure of β-ZnS phase (JCPDS card 77-2100). The cubic phase is stable at room temperature, while the hexagonal one is stable above 1020 °C [23]. Several groups [40–42] have reported the same result for ZnS films grown by chemical bath deposition. At pH=11 (Fig. 2e), a new peak has emerged at the diffraction angles of 31.53°, the latter corresponds to the plane (100) of ZnO hexagonal structure. Many works have shown that ZnS film contain a large amount of ZnO and $Zn(OH)_2$ [23,43]. The formation of ZnO after annealing can be due to film oxidation during annealing or to the thermal decomposition of $Zn(OH)_2$ already present in as grown film. This is in good agreement with the reported results by several groups [44–46]. The annealed films have a nanocrystalline structure. The crystallite size calculated from the XRD spectra, using Debye–Scherer [47] formula, are in the range 40–50 nm, this corresponds to varied full width at half maximum (FWHM) from 2.8 to 2.7×10^{-3} of ZnS intense peak (111).

3.3. Morphological properties

Fig. 3 shows two-dimensional AFM images for ZnS thin films. As can be seen films are dense and continuous. This is due to the second complexing agent hydrazine; it is well known that thiourea–ammonia bath yields to non uniform

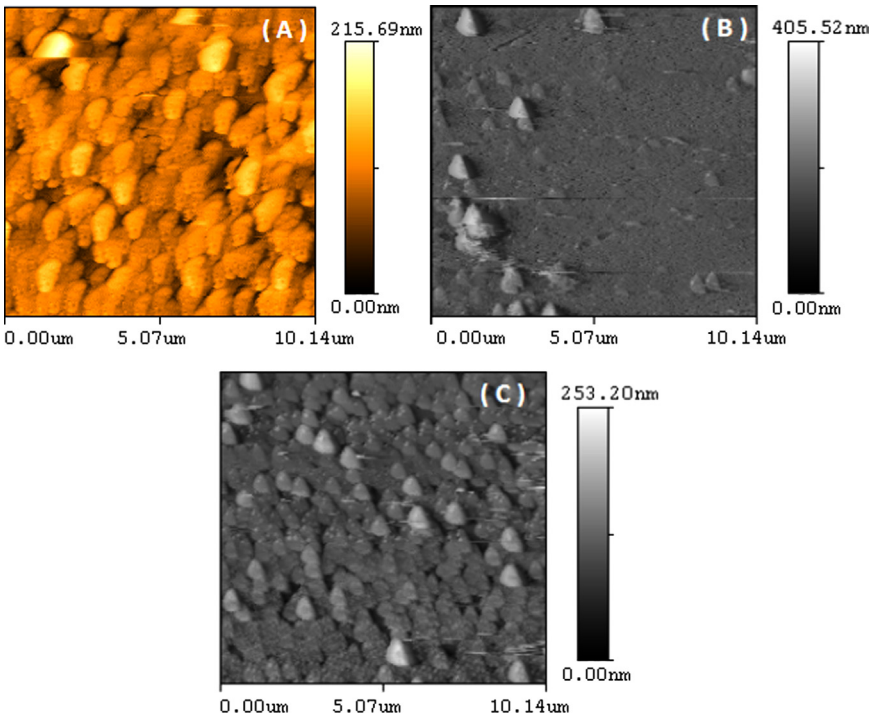

Fig. 3. AFM images of ZnS thin films deposited on glass substrate at different pH solutions. (a) pH 9, (b) pH 10 and (c) pH 10.66.

and non adherent film [31]. This justifies the popular large using of hydrazine as a second complexing agent [48]. It has been emphasized that adding hydrazine improves films homogeneity and growth rate [49]. The surface relief shows roughness and spherical crystallites uniformly distributed at pH 9 and 10.66 (Fig. 3a and c). However for film prepared at pH=10, the surface is smother; a discontinuous distribution of grains is observed on the film surface (Fig. 3b). The film surface morphology prepared at pH equal to 11 (not shown) is similar to that deposited one at pH equal to 9. In Fig. 4 we have reported the variation of film surface root mean square smoothness (Rq) estimated from AFM images. As seen, film prepared at pH=10 exhibit the smoother surface, this may due to: (i) the low deposition rate or to (ii) the large dissociation of ZnS at pH=10 [29]. The roughness is larger in film deposited at pH equal to 11, this rough film surface have favorable sites for H_2O adsorption which may lead to $Zn(OH)_2$ formation and explains the appearance of ZnO after annealing in this film, due to the decomposition of the adsorbed species. The measured average grain size, from AFM images, are ranged from 0.2 μm to 0.5 μm.

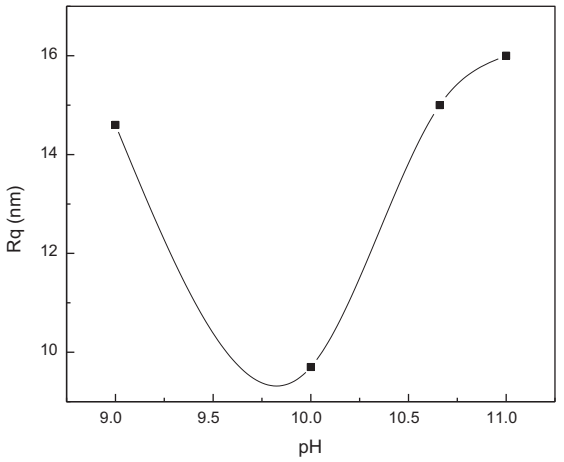

Fig. 4. Variation of ZnS thin films surface roughness as a function of pH solution.

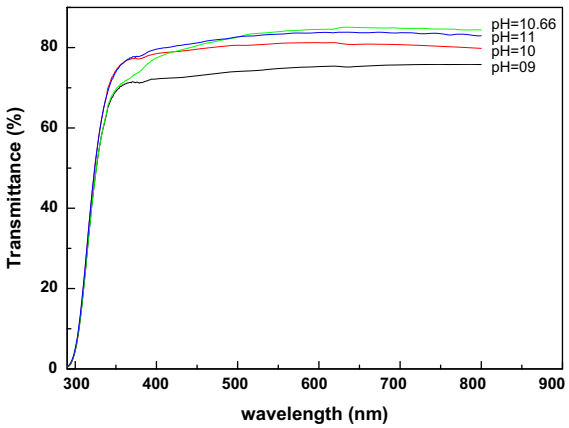

Fig. 5. Optical transmission spectra in the UV–visible region of ZnS film prepared with different pH.

3.4. Optical properties

Fig. 5 shows UV–vis transmittance spectra, in the range of 395–800 nm, of ZnS thin films prepared with different pH. The average transmittance values lies in between 75 and 80%. All the films have a steeper absorption around 300 nm. Optical band gaps of the films were obtained by using the Tauc formula [50]

$$(\alpha h\nu)^n = B(h\nu - E_g) \quad (8)$$

where B is a constant, E_g the band gap energy and n is equal to 2 for direct transition and 1/2 for indirect transition. Fig. 6 shows the plot of $(\alpha h\nu)^2$ versus photon energy $h\nu$ for the obtained ZnS films. The plots linearity indicates that the material is of direct band gap nature. The extrapolation of the straight line to $(\alpha h\nu)^2=0$ axis gives the energy band gap of the film material. The obtained optical bang gap (E_g) are reported in Fig. 7. The band gap energy are ranged from 4.0 eV to 4.2 eV for the deposited ZnS thin films. These values are rather larger than the literature value for the bulk ZnS (~3.68 eV).

The absorption coefficients of different samples exhibit a tail in the subgap photon energy region. The absorption tail width, well known as Urbach energy E_{00}, can be

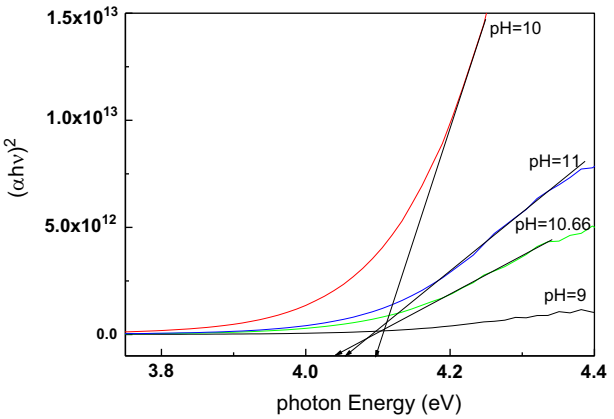

Fig. 6. Plot of $(\alpha h\nu)^2$ versus photon energy of different films used for optical gap determination.

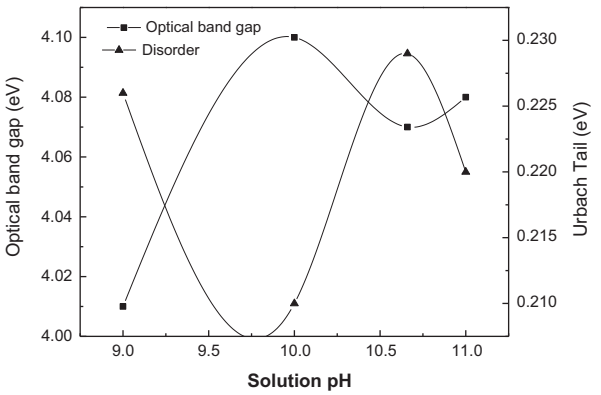

Fig. 7. Variation of optical gap and disorder in ZnS thin films network as a function of pH solution.

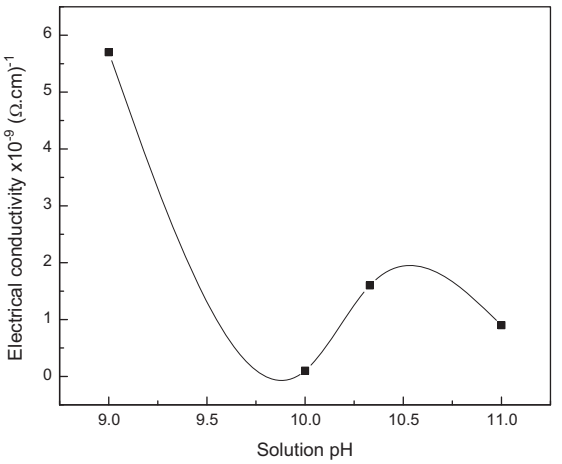

Fig. 8. Influence of pH solution on the electrical conductivity of ZnS thin films.

measured from the slope of plot of $\ln(\alpha)$ as a function of photon energy in the subgap absorption region. The latter is expressed as [51]

$$\alpha = \alpha_0 \exp[h\nu/E_{00}] \quad (9)$$

α_0 is a constant and E_{00} is the Urbach tail, it is also used as a signature of the disorder in the film network.

Fig. 7 shows the plot of band gap E_g and Urbach energy E_{00}, for ZnS films deposited at different pH. Film prepared with pH = 10 is less disordered films, this is due to the low deposition rate measured in this condition. This is consistent with the low surface roughness measured in this film. As can be seen, the variation of optical gap is opposite to the disorder. This behavior indicates clearly that the optical gap is also controlled by disorder in the film network.

3.5. Electrical properties

Films electrical properties were characterized by current–voltage (I–V) measurements. The measured conductivity values are reported in Fig. 8. As can be seen, the pH solution alters the film conductivity, the measured conductivities are ranged from 10^{-10} to 6×10^{-9} $(\Omega.\mathrm{cm})^{-1}$. The electrical conductivity values are much smaller compared to the reported one in bulk ZnS crystal [52]. The dark conductivity variation can be explained in terms of disorder in film network. The reduction in the conductivity is due to the increase in the disorder in films network. As seen in Fig. 5, films conductivity variation is opposite to Urbach tail one (Fig. 4). As mentioned above, Urbach tail width, also commonly known as disorder, originates from the deviation of distance and angle bond from their standard values in bulk material, this causes the appearance of valence and conduction band tails states [53]. More is disordered the film more is larger the Urbach tail. In a disordered structure, free carriers mobility and concentration are reduced due to the presence of large defects.

4. Conclusion

Nanocrystalline ZnS thin films were deposited on glass substrates by the CBD technique. The pH solution influence on films properties is investigated. Structural and morphological characterizations reveal that, as grown ZnS films are amorphous, while a thermal anneal at 550 °C, yields to a nanocrystalline material with a cubic structure (β-ZnS). The obtained ZnS films have a large band gap. The latter is governed by both the crystallite size and the disorder in film network. From the electrical and optical characterization, we inferred that using a solution with pH equal to 10 yields to ZnS films with optimal properties suitable for application as buffer layer in chalcogenide based thin film solar cells.

References

[1] S.H. Deulkara, C.H. Bhosalea, M. Sharonb, Journal of Physics and Chemistry of Solids 65 (2004) 1879.
[2] F. Göde, C. Gümüs, M. Zor, Journal of Crystal Growth 299 (2007) 136.
[3] J.A. Ruffner, M.D. Hilmel, V. Mizrahi, G.I. Stegeman, U. Gibson, Journal of Applied Optics 28 (1989) 5290.
[4] N. Fathy, R. Kobayashi, M. Ichimura, Materials Science and Engineering B 107 (2004) 271.
[5] J. Vidal, O. de Melo, O. Vigil, N. Lopez, G. Contreras-Puent, O. Zelaya-Angel, Thin Solid Films 419 (2002) 118.
[6] W. Tong, B.K. Wagner, T.K. Tran, W. Ogle, W. Park, C.J.J. Summer, Crystal Growth 164 (1996) 202.
[7] W.H. Bloss, F. Pfisterer, H.W. Schock, in: K.W. Boer, J.A. Duffie (Eds.), Advances in Solar Energy, An Annual Review of Research and Development, 4, American. Solar Energy Soc. Inc., New York, 1988, p. 275.
[8] K. Katsumi, Japanese Journal of Applied Physics 35 (1995) 4383.
[9] K. Ramanathan, M.A. Contreras, C.L. Perkins, S. Asher, F.S Hasoon, J. Keane, D. Young, M. Romero, W. Metzger, R. Noufi, J. Ward, A. Duda, Progress in Photovoltaics Research and Application 11 (2003) 225.
[10] M.A. Contreras, T. Nakada, M. Hongo, in: Proceedings of the 3rd World Conference of Photovoltaic Energy Conversion, 2000, p. 242.
[11] V. Dimitrova, J. Tate, Thin Solid Films 365 (2000) 134.
[12] A.E. Raid, F.D. Bvarlow, Thin Film Technology and Hand Book, Mc-Gaw Hill Compagny, New York, 1998.
[13] L.I. Maissel, R. Gland, Hand Book of Thin Film Technology, Mc Graw Hill Book Comapany, New York, 1970, pp. 230–240.
[14] M. Gunasekaran, R. Gopalakrishnan, P. Ramasamy, Materials Letters 58 (2003) 67.
[15] C.D. Lokhande, A. Ennaoui, P.S. Patil, M. Giserg, K. Diesner, H. Tributsch, Thin Solid Films 330 (1998) 70.
[16] S. Yamaga, A. Yoshokawa, H. Kasain, Journal of Crystal Growth 86 (1998) 252.

[17] M. Tonouchi, S. Yong, M. Tarsuro, M. Hirosh, O. Masaki, Journal of Applied Physics 2L (1990) 2433.
[18] P.J. Dean, A.D. Pitt, M.S. Skolnick, P.J. Wright, B. Cockayne, Journal of Crystal Growth 5 (1982) 9301.
[19] J. Cheng, D.B. Fan, H. Wang, B.W. Liu, Y.C. Zhang, H. Yan, Semiconductor Science and Technology 18 (2003) 676.
[20] D.A. Johnstona, M.H. Carlettoa, K.T.R. Reddyb, I. Forbesa, R.W. Miles, Thin Solid Films 403–404 (2002) 102.
[21] R. Sahraei, G. Motedayen Aval, A. Goudarzi, Journal of Alloys and Compounds 466 (2008) 488.
[22] M. Dhanam, B. Kavitha, Chalcogenide Letters 7 (2009) 299.
[23] F. Long, W.M. Wanga, Z. Cui, L. Fan, Z. Zou, T. Jia, Chemical Physics Letters 462 (2008) 84.
[24] P. Roy, J.R. Ota, S.K. Srivastava, Thin Solid Films 515 (2006) 1912.
[25] P. Uday Bhaskar, G. Suresh Babu, Y.B. Kishore Kumar, Y. Jayasree, V. Sundara Raja, Materials Chemistry and Physics 134 (2012) 1106.
[26] R. Sahraei, G. Motedayen Aval, A. Baghizadeh, M. Lamehi-Rachti, A. Goudarzi, M.H. Majles Ara, Materials Letters 62 (2008) 4345.
[27] Q. Liua, M. Guobinga, A. Jianpingb, Applied Surface Science 254 (2008) 5711.
[28] T. Ben Nasr, N. Kamoun, M. Kanzari, R. Bennaceur, Thin Solid Films 500 (2006) 4.
[29] C. Hubert, N. Naghavi, B. Canava, A. Etcheberry, D. Lincot, Thin Solid Films 515 (2007) 6032.
[30] K. Ernits, K. Muska, M. Danilson, J. Raudoja, T. Varema, O. Volobujeva, M. Altosaar, Advances in Materials Science and Engineering;2009 http://dx.doi.org/10.1155/2009/372708. ID 372708.
[31] D. Lincot, R. Ortega-Borges, Journal of the Electrochemical Society 139 (1992) 1880.
[32] B.S. Rema Devi, R. Raveendran, A.V. Vaidyan, PRAMANA. cO Indian Academy of Sciences 68 (2007) 679.
[33] J.M. Dona, J. Herrero, Journal of the Electrochemical Society 141 (1994) 205.
[34] D.A. Johnston, M.H. Carletto, K.T.R. Reddy, I. Forbes, R.W. Miles, Thin Solid Films 403–404 (2002) 102.
[35] Q. Liu, M. Guobing, A. Jianping, Applied Surface Science 254 (2008) 5711.
[36] P. Roy, J.R. Ota, S. Kumar Srivastava, Thin Solid Films 515 (2006) 1912.
[37] J. Vidal, O. de Melo, N. Lopez, O. Zelaya-Angel, Materials Chemistry and Physics 61 (1999) 139.
[38] D.A. Johnston, M.H. Carletto, K.T.R. Reddy, I. Forbes, R.W. Miles, Thin Solid Films 403–404 (2002) 102.
[39] J. Cheng, D.B. Fan, H. Wang, B.W. Liu, Y.C. Zhang, H. Yan, Semiconductor Science and Technology 18 (2003) 676.
[40] S.D. Sartale, B.R. Sankapal, M. Lux-Steiner, A. Ennaoui, Thin Solid Films 480–481 (2005) 168.
[41] J. Lee, S. Lee, S. Cho, S. Kim, I.Y. Park, Y.D. Choi, Materials Chemistry and Physics 77 (2002) 254.
[42] P. Roy, J.R. Ota, S.K. Srivastava, Thin Solid Films 515 (2006) 1912.
[43] A. Goudarzi, G.M. Aval, R. Sahraie, Thin Solid Films 516 (2008) 4953.
[44] J. Cheng, D. Bo, H.W. Fan, Electron Journal 18 (2003) 676.
[45] K. Kushiya, Solar Energy 77 (2004) 717.
[46] S. Kundu, C.O. Larry lsen, Thin Solid Films 471 (2005) 298.
[47] H.P. Klung, L.E. Alexander, X-Ray Diffraction Procedures for Polycrystalline and Amorphous Materials, 2nd edition, Wiley, New York, 1974, p. 220.
[48] C.D. Lokhande, P.S. Patil, H. Tributsch, A. Ennaoui, Solar Energy Materials and Solar Cells 55 (1998) 379.
[49] J.M. Dona, J. Herrero, Journal of the Electrochemical Society 144 (1997) 4081.
[50] J.J. Tauc, Amorphous and Liquid Semiconductor, Plenum, New York, 1976, p. 169.
[51] M.V. Kurik, Physica Status Solidi A 8 (1971) 9.
[52] C. Elbaum, Physical Review Letters 32 (7) (1974) 376.
[53] F. Urbach, Physical Review 92 (1953) 1324.